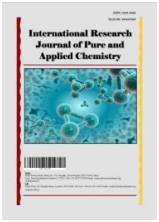

International Research Journal of Pure & Applied Chemistry

22(5): 36-53, 2021; Article no.IRJPAC.69583
ISSN: 2231-3443, NLM ID: 101647669

Adsorption of Water Contaminates by $MnFe_2O_4$ Nano Particles

Yousra Hamdy Farid[1*]

[1]Basic Science Department, Alexandria Higher Institute for Engineering and Technology (AIET), Alexandria, Egypt.

Authors' contributions

The sole author designed, analyzed, interpreted and prepared the manuscript.

Article Information

DOI: 10.9734/IRJPAC/2021/v22i530408
Editor(s):
(1) Prof. A. V. Raghu, Jain University, India.
(2) Prof. Bengi Uslu, Ankara University, Turkey.
(3) Prof. Wolfgang Linert, Vienna University of Technology, Austria.
Reviewers:
(1) S.Sharmila, Bharath Institute of Higher Education and Research, India.
(2) Takashiro Akitsu, Tokyo University of Science, Japan.
Complete Peer review History: https://www.sdiarticle4.com/review-history/69583

Original Research Article

Received 25 April 2021
Accepted 02 July 2021
Published 10 July 2021

ABSTRACT

Wastewater treatment and reuse is a critical issue, researchers are trying to find for cheap and reasonable advances. Adsorption is the most important strategy to evacuate heavy metals. Adsorption happens when particles diffused within the liquid stage for a period of time using the force radiating from an adjoining surface. Nickel and eosin yellow removal from industrial wastewater is considered utilizing manganese ferrite (MnFe2O4), nano particles (Nps), extracted by a co-precipitation strategy at room temperature. The variables examined are the contaminant concentration, weight, pH and contact time. Adsorption isotherm models is examined. The results reveal that the nano manganese ferrite could be adopted as a great adsorbent for the evacuation of nickel and eosin yellow from contaminated water. It is shown that the particle removal rate is diminished with an increment in initial concentration. Also, it shows as the pH increases in the water, the higher the percent removal of the contaminants. Then, it is discovered that as the adsorbent dose is increased from 1 to 3 g/l, the removal of Ni+2 increases from 37% to 60%. The removal of eosin yellow increases from 12% to 28% with an increment within the adsorbent dose from 1 to 4 g/l. The results show that adsorption using nano particles is physiosorption (physical sorption) that occurs at room temperature. The results also revealed that (MnFe2O4), nano particles was a promising adsorbent for removal of Ni ions from industrial wastewater.

**Corresponding author: E-mail: eng_yousra_hamdy@yahoo.com, dr.yousra.hamdy@aiet.edu.eg;*

Keywords: Adsorption; wastewater; Nickel; eosin yellow dye; nano particles.

ABBREVIATIONS

(NPs) : Nano particles.
(SEM) : Electron microscopy.
(FTIR) : Fourier Transform Infra-Red.
(XRD analysis) : X-Ray Diffraction.

NOMENCLATURE

B : Constant related to the adsorption energy ($mol^2 J^2$).
b : Langmuir constants, related to the binding constant (L mg^{-1}).
c : Constant.
C_e : Equilibrium concentration of the Ni (II) in solution (mg L^{-1}).
E : Free energy change (kJ mol^{-1}).
K : Reaction rate constant.
K_F : Freundlich constant; related to the bonding energy.
k_d : Intra-particle diffusion rate constant (mg g^{-1} $min^{-0.5}$).
NPs : Nano particles.
q_e : Adsorption capacity at equilibrium (mg g^{-1}).
q_{max} : Maximum adsorption capacity (mg g^{-1}).
q_t : Amount of adsorbed Ni(II) (mg g^{-1}).
Q_m : Theoretical saturation capacity (mg g^{-1}).
t : Time (s).
ε : Polanyi potential.

1. INTRODUCTION

There are various sources of industrial wastewater, however they are all plants of some kind producing different products, and the type of the waste in the water depends on the industry itself., like Organic chemical industry, Food industry, Electric power plants, and Iron and steel industry.

Industrial wastewater should be treated with various methods depending on the contaminants itself and the environment regulations that are required to be met.

Water pollutants divided into two categories:

1. Inorganic pollutants like: Heavy metals, Acidity discharges, Chemical waste, Fertilizers from agricultural use, and Silt from construction sites, logging, slash and burn operation.
2. Organic pollutants like: Insecticides and herbicides, Bacteria from livestock operations, Food processing waste , Tree debris from logging operations, VOCs including solvents and hydrocarbons, and Detergents and chemical compounds found in cosmetics products.

Heavy metals are naturally occurring elements that are found throughout the earth's crust, most environmental contamination and human exposure result from anthropogenic activities such as mining and smelting operations, industrial production and use, and domestic and agricultural use of metals and metal-containing compounds. Environmental contamination can also occur through metal corrosion, atmospheric deposition, soil erosion of metal ions and leaching of heavy metals, sediment re-suspension and metal evaporation from water resources to soil and ground water. Natural phenomena such as weathering and volcanic eruptions have also been reported to significantly contribute to heavy metal pollution [1].

In particular, the discharge of dye-containing effluents into the water environment is undesirable because of their color, released directly and breakdown products are toxic, carcinogenic or mutagenic to life forms mainly because of carcinogens such as benzidine, naphthalene are other aromatic compounds.

Dyes leads to number of environmental & health hazards which are as follows:

1. The greatest environmental concern which dyes is their absorption and reflection of sunlight entering the water. Light absorption diminishes photosynthetic activity of algae and seriously influences the food chain.
2. Many dyes and their breakdown products are carcinogenic, mutagenic and/or toxic to life. Dyes are mostly introduced into the environment through industrial effluents.
3. Triple primary cancers involving kidney, urinary bladder and liver of dye workers have been reported.
4. Textile dyes can cause allergies such as contact dermatitis and respiratory diseases, allergic reaction in eyes, skin irritation, and irritation to mucous membrane and the upper respiratory tract.
5. Reactive dyes from covalent bonds with cellulose, woolen and PA fibers. Certain reactive dyes have caused respiratory

sensitization of workers occupationally exposed to them.

6. The presence of very small amounts of dyes in the water, which are nevertheless highly visible, seriously affects the quality and transparency of water bodies such as lakes, rivers and others, leading to damage to the aquatic environment.
7. The highly toxic and mutagenic dyes decrease light penetration and photosynthetic activity, causing oxygen deficiency and limiting downstream beneficial uses such as recreation, drinking water and irrigation.
8. Azo dyes have toxic effects, especially carcinogenic and mutagenic. They entering the body by ingestion and are metabolized by intestinal microorganisms causing DNA damage. [2]

Eosin is a name of several fluorescent acidic compounds which bind to and from salts with basic, or eosinophilic, compounds like proteins containing amino acid residues such as arginine and lysine, and stains them dark red or pink as a result of the actions of bromine on fluorescein. In addition to staining proteins in the cytoplasm, it can be used to stain collagen and muscle fibers for examination under the microscope. Structures that stain readily with eosin are termed eosinophilic.

Eosin is a water soluble dye, a “red crystalline powder, designated by the formula C20H8O5Br4, used in textile dyeing and ink manufacturing” or “the red sodium salt of this powder, used in biology to stain cells”, or “any of a class of red acid dyes of the xanthene group used as cytoplasmic stains and as counter-stains.

Eosin is an orange-pink dye with wave length of 416 nm … used to stain cytoplasm, collagen and muscle fibers for examination under the microscope. [3]

There are different strategies to remove heavy metals and natural contaminations from fluid solutions. These include chemical precipitation, reverse osmosis, adsorption, membrane partition, electrochemical strategies, and ion exchange. [4] Adsorption is one of the first recommended physicochemical treatment types. In adsorption, the gas or liquid particles bind to the solid or liquid surface that is termed the adsorbent, the particles form an atomic or molecular adsorbate film. Isotherms are used to describe adsorption because temperature has a significant effect on the process. The quantity of adsorbate bound to the adsorbent is expressed as a function of pressure of concentration at constant temperature. Several isotherm models have been developed to describe adsorption, including the linear, Freundlich, Langmuir, BET (after Brunauer, Emmett, and Teller), and Kisliuk theories [5].

Adsorption characteristics like fundamental operation, speedy response, and low cost. Industrial by-products, like fly ash remains, iron slags, hydrous titanium oxide, can be chemically modified to boost their effect in metal removal from waste water.

Fly ash debris is explored as adsorbents for the removal of destructive metals. [6]

Previous studies about the utilization of adsorbents and adsorption procedures in heavy metal removal from wastewater, for the reason of finding a reasonable, compelling, and broadly related methodology that makes the smallest amount of sludge. These adsorbents utilized in adsorption techniques may consolidate manufactured or ordinary zeolites, bio-sorbents, clay minerals, activated carbon, fly ash remains, hydrogels, and nanoparticles. Nano-materials, such as nano-metal oxides include iron oxides, manganese oxides, aluminum oxides, CuO, NiO, ZnO and TiO2 , carbon nanotubes, and appealing nanoparticles, have been examined as accessible materials to be utilized for the adsorption of heavy metals due to their unique characteristics, high adsorption capacity and unsaturated surfaces [7-15].

The surface of magnetic manganese ferrite nanoparticles (MFN) was modified using cetyl trimethylammonium bromide (CTAB). The modified MFN was investigated for dye removal for single and ternary systems. The adsorption kinetic for the dyes was found to be well described by the pseudo-second order model. The maximum dye adsorption capacity (Q0) of MFN-CTAB for DR80, DR31 and AB92 was 83 mg/g, 59 mg/g and 70 mg/g, respectively. The adsorption isotherm data were analyzed using the Langmuir, Freundlich, and Temkin equations. The results revealed that the Langmuir model fitted the adsorption data better. The results showed that the MFN-CTAB as a magnetic adsorbent might be a suitable alternative to remove dyes from colored aqueous solutions [16].

Magnesium ferrite has attracted attention as one of the ferrites for high density magnetic recording, microwave absorbents, sensors and electronic device, high frequency devices, color imaging, v/m nbvb and so forth, because it has high magnetic permeability and high electrical resistance .It has a cubic structure of normal spinel-type and is a soft magnetic semiconducting material.

Also Magnetic Magnesium Ferrite has been reported to show a large temperature rise under magnetic field, and it's not toxic to human cells, therefore it has been used in medicine as cancer therapy as it can deliver the required dose of the toxic drugs to the affected tissues due to its magnetic properties without harming any other cells.

It can also be used as an adsorbent for waste water treatment.

The synthesis of Nano manganese oxides (MONs) was studied by the prepared MONs, Further, and the adsorption of nickel from aqueous solution was studied kinetically to explore and understand the adsorption mechanism.

Nanostructured materials have recently been proposed as effective, low-cost, and ecologically-inviting elective adsorbents to existing treatment materials.

In the study at hand, the removal of total Nickel and Eosin yellow from factories' wastewater is considered via the use of manganese ferrite ($MnFe_2O_4$) Nano particles (NPs) which are synthesized by adopting a co-precipitation strategy at room temperature beneath batch conditions [17].

The aims of this study are:

1. Description of Preparation of Nano-manganese ferrite particles.
2. Identifying obstacles and factors that would hinder successful of Nickel and Eosin yellow removal from wastewater.

2. MATERIAL AND METHODOLOGY

2.1 Methodology Steps:

1. Analysis of Manganese oxide was done by Fourier Transform Infra-Red [FTIR], Scanning Electron Microscopy [SEM], and X-Ray Diffraction analysis [XRD]
2. The effect of the following factors is studied regarding the removal of Nickel ions and Eosin Yellow Dye from industrial contaminated water: The influence of concentration, the influence of weight, and the influence of pH.
3. Kinetics of adsorption was studied for intra-particle diffusion to show the quantity of adsorbed Ni ions and Eosin Yellow Dye.
4. The statistical analysis was done by using plotting charts in excel sheets.

2.2 Materials and Tools

2.2.1 Devices used

Stirrer, Water bath, pH Meter, Drying Oven, and Muffle Furnace

2.2.2 Materials

1. Ferric Chloride Hexahydrate, $FeCl_3.6H_2O$, MP Biomedicals, with 97% purity.
2. Manganese Chloride Tetrahydrate. $MnCl_2{\cdot}4H_2O$, Alfa Aesra, with 99.99% purity.
3. Caustic Soda.Egyptain petrochemical co, solution 48-50% conc.
4. Oleic Acid.C18H34O2, Malysia.
5. Distilled Water.
6. Nickel Chloride. Lubon Industry Co. with 98 % purity.
7. Eosin Yellow. SPI –CHEM, $C_2OH_6Br_4Na_2O_5$.

2.2.3 Preparation of nano-manganese ferrite particles [17]

a) Weigh 27.045 g of ferric chloride hexahydrate and put them in 250 ml of deionized water to prepare (0.4M) of ferric chloride solution.
b) Weigh 2.473 g of manganese chloride tetrahydrate and put them in 250 ml of refined water to induce prepared (0.2M) of manganese chloride solution
c) Include 13.1 ml of caustic soda to 250 ml of deionized water to arrange (3M) solution.
d) Blend the ferric chloride solution and the manganese chloride solution and next slowly incorporate the yielded mix to 3M caustic soda solution by mixing at 1000 rpm for 1 hour and a half to induce a mix of pH from 11 to 13.
e) Put the colloidal solution in a water bath at 90°C for 120 minutes to ensure that the

NaCl is removed from the powder.

f) Wash the resulting solution 10 times with hot deionized water until the filtrate has a pH 7.
g) Dry the filtrate in a drying stove at 80°C for 2 h.
h) The precipitate is at that point calcined at 700 °C for 4 hours in a muffle oven.

2.3 Theoretical framework: Definitions and concepts

2.3.1 Adsorption isotherm

The foremost recognized surface adsorption models for single-solute frameworks are the Langmuir and Freundlich models.

2.3.2 The langmuir isotherm

Utilizing the Langmuir isotherm condition, the adsorption information is substituted within the taking after linearized form:

$$\frac{C_e}{q_e} = \frac{1}{q_{max}\, b} + \frac{1}{q_{max}} C_e \quad (1)$$

Where C_e is the equilibrium concentration of the Ni (II) in solution (mg L-1), q_e is the adsorption capacity at equilibrium (mg g-1), b is (L mg-1) Langmuir constants, related to the binding constant and q_{max} (mg g-1) is the maximum adsorption capacity. A plot of specific sorption (C_e/q_e) vs. Ce yields a straight line of slope ($1/q_{max}$) and intercepts ($1/q_{max}$ b), as shown in Table 1. [18]

2.3.3 The freundlich isotherm

Using the following non-linear equation, the Freundlich isotherm is represented by:

$$qe = K_F\, Ce^{1/n} \quad (2)$$

K_F is characterized as the adsorption or conveyance coefficient showing the amount of Ni^{2+} adsorbed onto adsorbent for unit equilibrium concentration. 1/n demonstrates the adsorption intensity of Ni2+ onto the sorbent with surface heterogeneity, getting to be more heterogeneous as its value approaches zero. Eq. (2) can be linearized based on the logarithmic. Eq. (3) and the Freundlich constants can be calculated by:

$$\log q_e = \log K_F + \frac{1}{n} \log C_e \quad (3)$$

Utilizing the same set of test information, the pertinence of the Freundlich sorption isotherm is inspected by plotting log (q_e) vs. log (C_e). The information gotten from the linear Freundlich isotherm plot for the adsorption of Ni 2+ on Manganese ferrite is shown in Table1. The relationship coefficients detailed in Table 1 appear distinctive confirmation that the adsorption of Ni^{2+} onto Manganese Ferrite takes after the Freundlich isotherm for 100ppm Ni^{2+} concentration. Whereas the adsorption of Eosine color onto Manganese Ferrite takes after the Langmiur isotherm for 50 ppm dye concentration [19].

The Dubinin–Radushkevich (D–R) isotherm; D–R show; is assist utilized to calculate the porosity of the adsorbent, the apparent energy of adsorption and the characteristics of adsorption on micropores rather than those on a layer-by-layer adsorption [7,17].

The D–R model has often been used in the following Eq. (4) and its linear form can be expressed in Eq. (5)

$$q_e = Q_m \exp(-B\varepsilon^2) \quad (4)$$

$$\ln q_e = \ln Q_m - B\varepsilon^2 \quad (5)$$

Where B is a constant related to the adsorption energy ($mol^2\ J^2$), Qm the theoretical saturation capacity (mg g-1), and ε the Polanyi potential, calculated from Eq. (6).

$$\varepsilon = RT \ln (1+1/Ce) \quad (6)$$

The slope of the plot of ln q_e vs. ε^2 gives B (mol^2 (kJ^2) −1) and the intercept gives the adsorption capacity; Q_m (mg g−1). The mean free energy of adsorption, E (kJmol-1), characterized as the free energy change when one mole of particle is exchanged from interminability withi n the fluid stage to the surface of the solid within the solution, is calculated from the B value using Eq (7). [20]

$$E = 1/\sqrt{(-2B)} \quad (7)$$

Table 1. Langmuir and Freundlish models data for the removal of Ni (II) and Eosin dye onto Manganese Ferrite using batch reactor

Isotherm model	Ni(II)	Eosin dye
Langmuir		
Q_0 (mg g-1)	22.271	2.5445
K_a (L mg-1)	0.1624	0.0684
No. of parameter estimated	2	2
Data point available	4	4
R^2	0.9005	0.8644
Freundlich		
1/n	0.3356	0.4006
KF (mg g-1)	5. 6576	0.4270
No. of parameter estimated	2	2
Data point available	4	4
R^2	0.9679	0.9787

It is received to discover out the adsorption type. If the value is in the range 8-16 kJ mol−1 then ion exchange accounts for the adsorption type, and when E < 8, the adsorption type is physiosorption. [21,22] The value of E calculated utilizing Eq. (7) is 0.5 kJ mol−1 for Manganese ferrite. This demonstrates that the type of adsorption within hand is physiosorption (physical sorption) which regularly happens at low temperature. [23,24]

3. RESULTS AND DISCUSSION

3.1 The Characteristics of the Prepared Manganese Oxide

3.1.1 FTIR [Fourier Transform Infra-Red]

The FT-IR spectra of the prepared Manganese ferrite test within the range of 500 – 4000 cm-1 are revealed in Fig. 1. The band at 875 cm−1 is a common characteristic of all ferrites. The unique peak at 565 cm-1 is similar to the characteristic vibrations of the metal oxygen at the octahedral and tetrahedral destinations individually. [25]

Based on Josyulu and Sobhanadri [26], the powerless assimilation band at circular 350 and 360 cm-1 stems from a magnesium oxygen extending vibration on the octahedral location. The strong peak at 1633 cm-1 and 3800 cm-1 can be accounted for by the extending vibrations of the OH group [27].

3.1.2 SEM [Scanning Electron Microscopy]

A morphological investigation of Manganese ferrite is performed by checking electron microscopy (SEM) for the purpose of the most significant properties and morphology of the powders.

Fig. 2 illustrates the morphological Manganese Ferrite appearance and it shows that the item particles are consistently conveyed and are basically comprised of round particles with a normal grain measure of 93. [28]

BET surface area=16.0440 m2/g

Micropore volume=0.004314 cm3/g

3.1.3 XRD analysis [X-Ray diffraction]

Fig. 3 shows the X-beam diffraction design for the arranged manganese oxide particles. The XRD pattern and crystal phase structure of Mn doped $MnFe_2O_4$ with diffraction peaks at 2θ = 30.09°, 35.35°, 42.93°, 53.22°, 56.81°, 62.32°, 70.68°, 73.70°, and 78.43° shown in Fig. 3 were conclude the cubic spinel phase of MnFe2O4 . The chart indicating the transition from (Mn, Fe)O to $MnFe_2O_4$, which is in accordance with the nature of the redox reaction. No diffraction peaks related to MgO and FeOx were observed, indicating that the ferrites structures did not collapse after reaction and all the ferrites could return to their original state with good regenerability. The cross section parameter values concur with those calculated by Yihan, et al. [29]

3.2 The Influence of Contact Time

Nickel chloride is prepared with different concentrations as follow:

1. 1000 ppm nickel solution is arranged by dissolving 4.04 g of hydrated nickel chloride in 1000ml of deionized water.

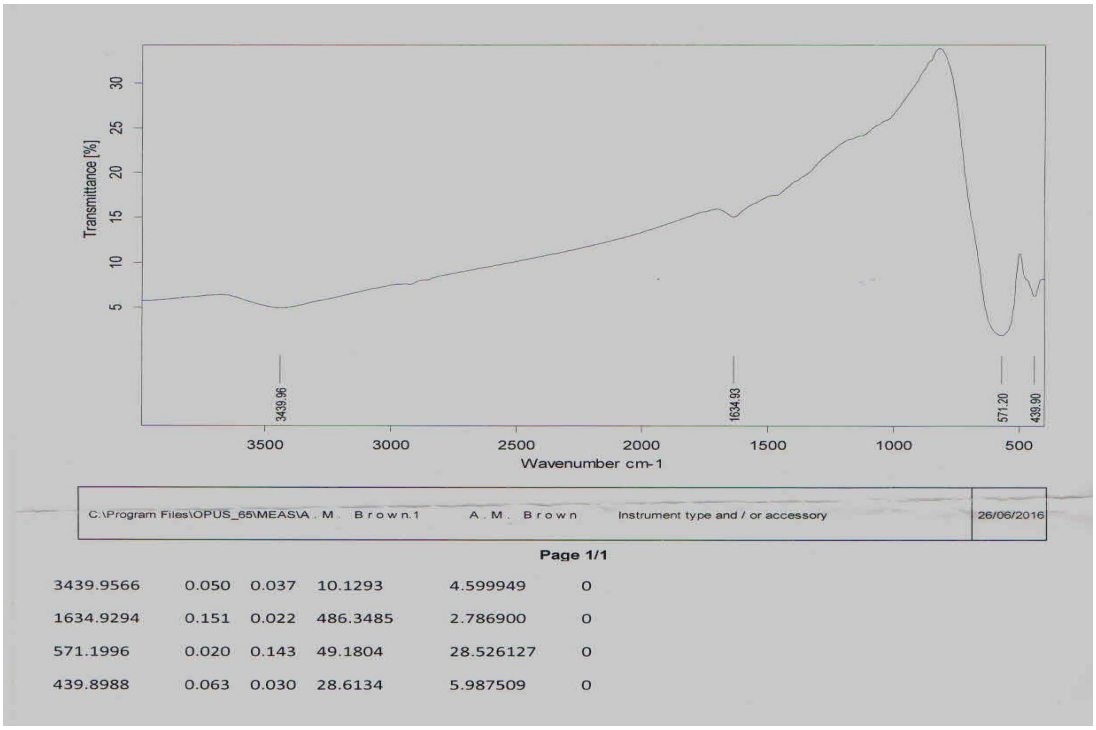

Fig. 1. FTIR for Manganese ferrite

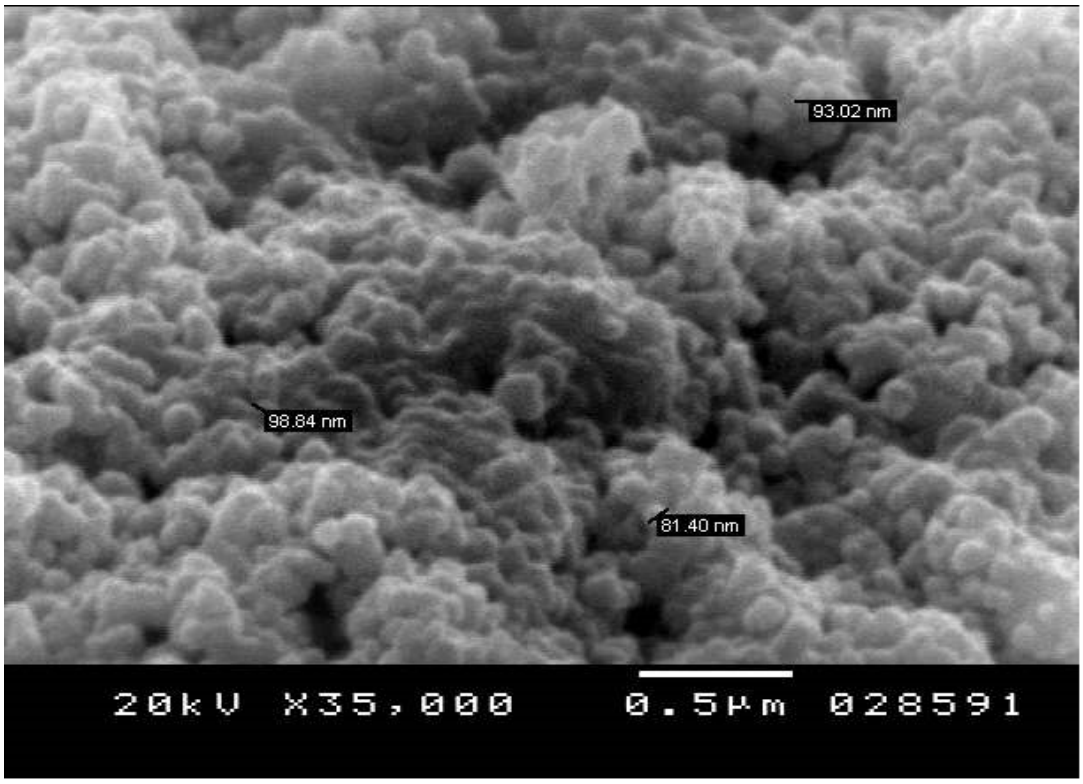

Fig 2. SEM for manganese ferrite

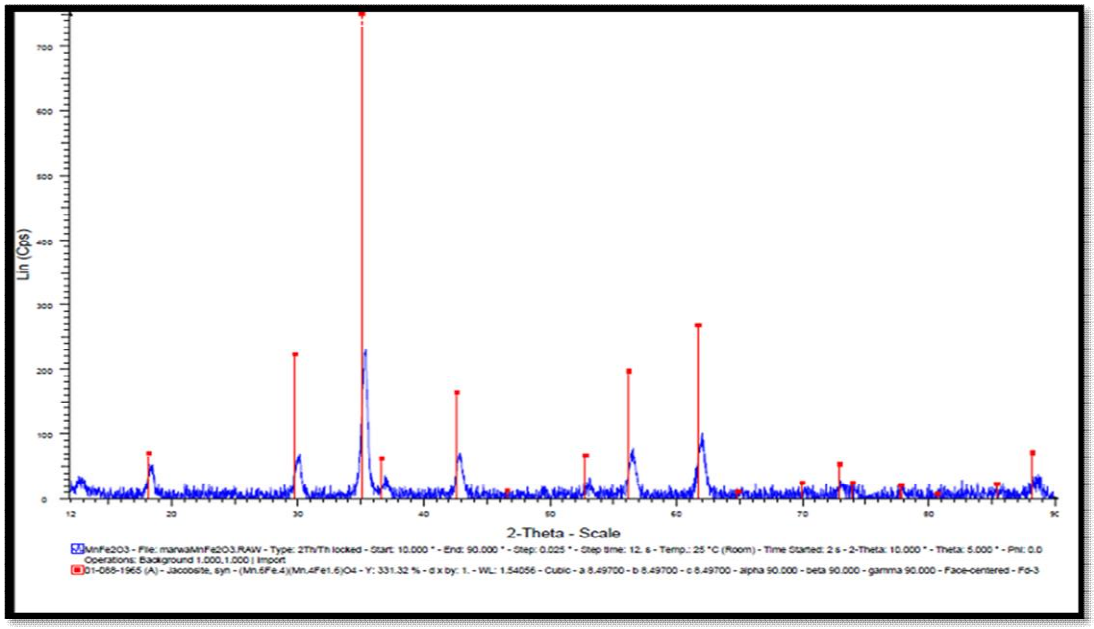

Fig. 3. XRD analysis of Manganese ferrite

2. 1100 ml of 100 ppm nickel chloride solution is arranged, and 11 bottles are prepared for pouring 100 ml of 100 ppm solution in each one.
3. 0.1 g of manganese ferrite is added to 10 bottles, at that point the bottles are put in a shaker working at 220 rpm and one bottle is pulled back after 5, 10, 15, 20, 25, 30, 45, 60, 75 and 90 minutes individually for analysis.
4. The previous steps are then repeated for 75, 50 and 25 ppm solution.

Different concentrations of methylene yellow are prepared as follow:

1. 1000 ppm color solution is arranged by dissolving 1 g of methylene yellow in 1000ml of deionized water.
2. 1100 ml of 50 ppm methylene yellow solution is arranged, at that point, in 11 bottles, 100 ml of 50 ppm solution is put in each one.
3. 0.2 g of manganese ferrite is added to 10 bottles. Next, the bottles are placed in a shaker working at 220 rpm and they are pulled back after 5, 10, 15, 20, 25, 30, 45, 60, 75 and 90 minutes individually for analysis.
4. The previous steps are repeated for a 25, 20 and 10 ppm solution.

The influence of time on the adsorption of Ni^{2+} (100 ppm) utilizing a batch reactor is shown in Figs. 4 to 8. The removal percentage of Ni^{2+} is proven to be 38%, 46%, 53% and 82 % for 100 ppm, 75 ppm, 50 ppm and 25 ppm Ni^{2+} individually by utilizing 2g/l Manganese ferrite Nano-powder for 90 min. [30]

It is shown that the Ni^{2+} adsorption is fast at the beginning of the adsorption. It is then gradually expanded with time, getting nearly steady after 1 and a half hour. This feature can be explained by the fact that vacant places are found in the beginning of the adsorption process. Then, an increase in the repulsive forces takes place, caused by the existence of the adsorbed ions, making the remaining positions more troublesome to get to. [31,32] It is noticeable that the particle removal rate is diminished with an increment in the initial concentration.

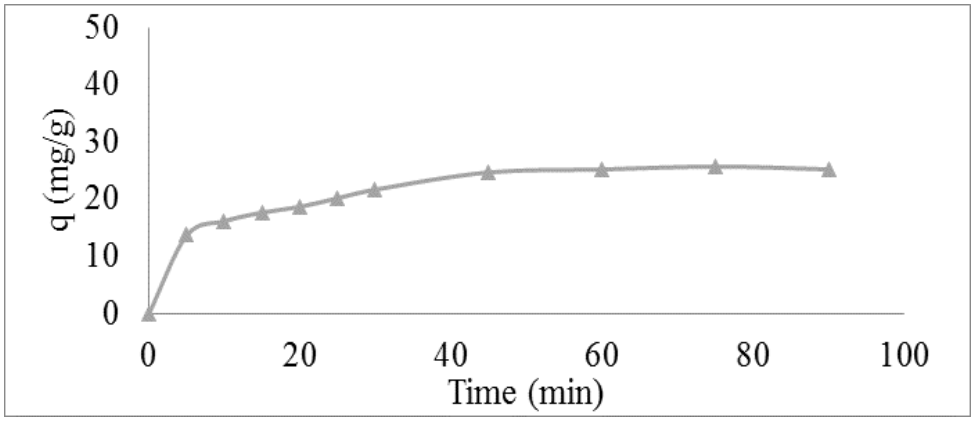

Fig. 4. Influence of contact time on the adsorption capacity of (Manganese ferrite) for Ni ions at 100 ppm concentration and 6 pH, adsorbent dosage 2 g/l and temperature 25°C

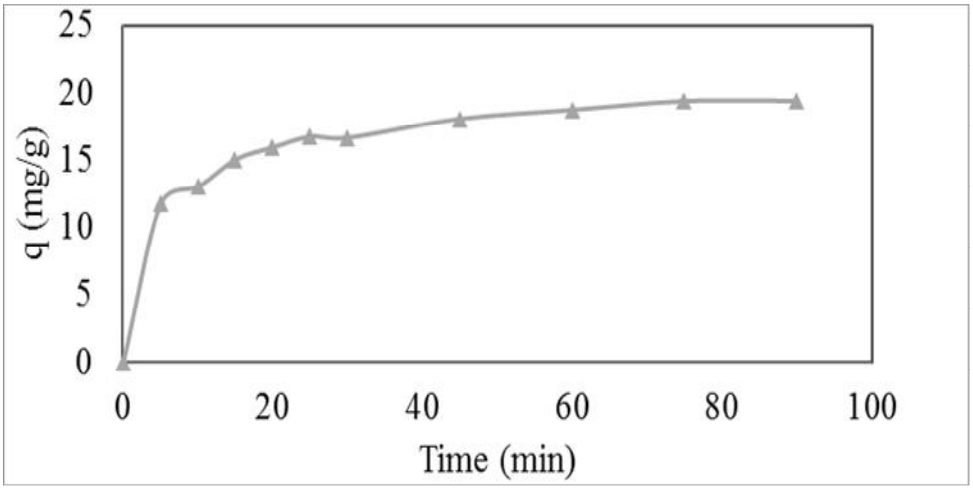

Fig. 5. Influence of contact time on the adsorption capacity of (Manganese ferrite) for Ni ions at 75 ppm concentration and pH 6, adsorbent dosage 2 g/l and temperature 25°C

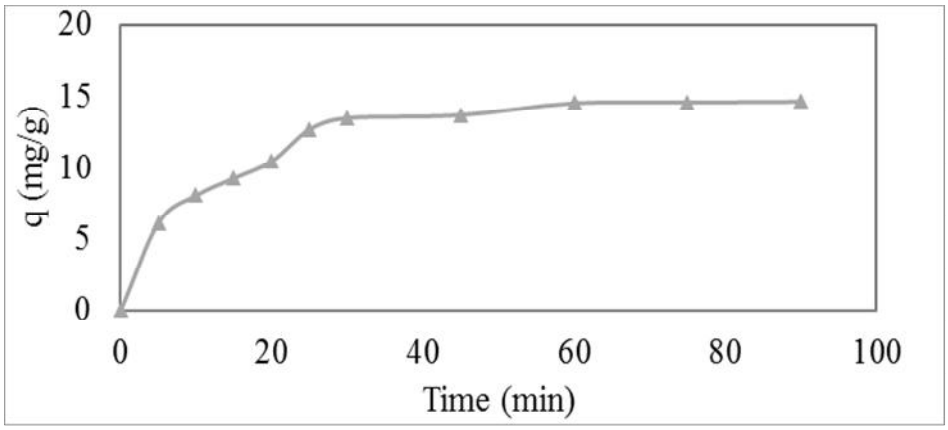

Fig. 6. Influence of contact time on the adsorption capacity of (Manganese ferrite) for Ni ions at 50 ppm concentration and pH 6, adsorbent dosage 2g/l and temperature 25°C

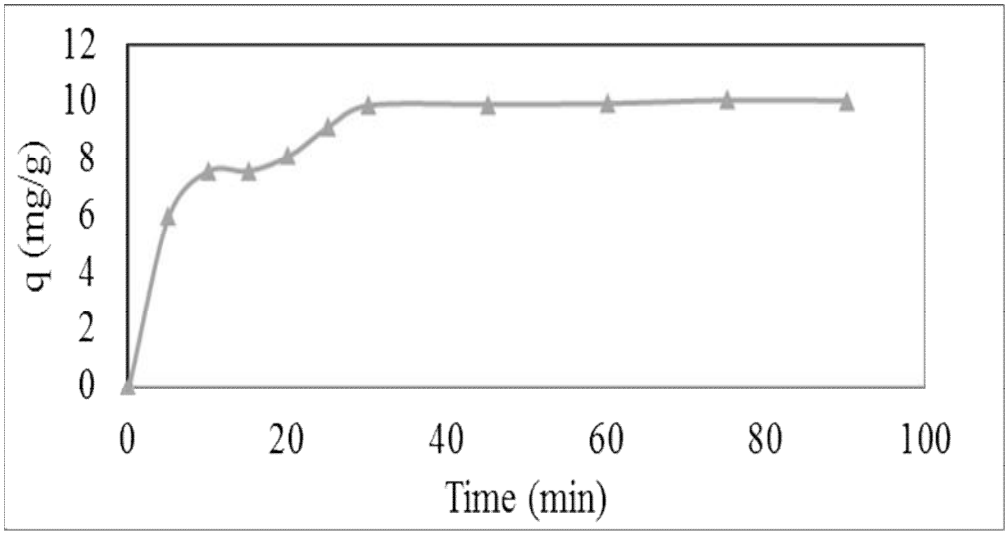

Fig. 7. Influence of contact time on the adsorption capacity of (Manganese ferrite) for Ni ions at 25 ppm concentration and pH 6, adsorbent dosage 2 g/l and temperature 25°C

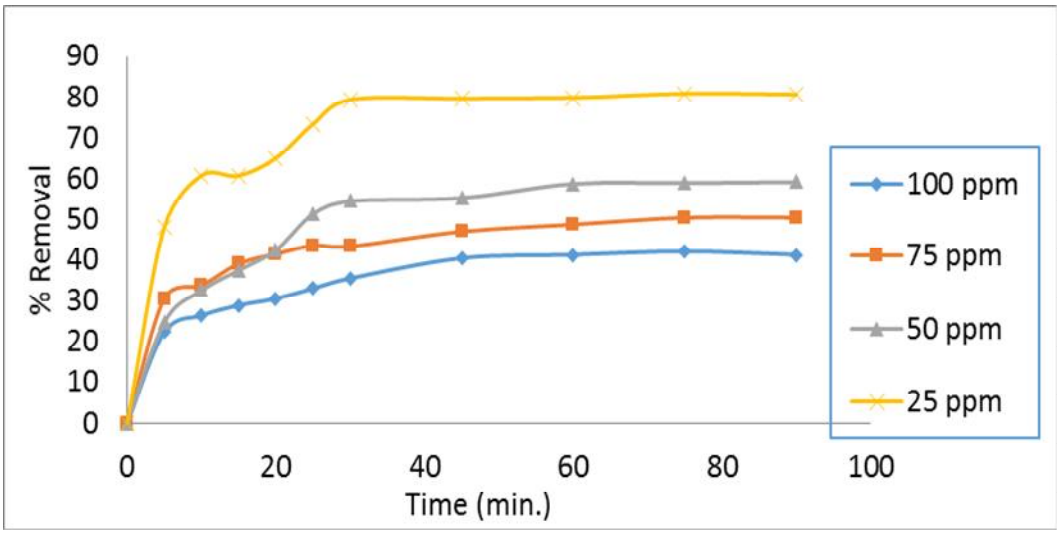

Fig. 8. Influence of contact time and Ni concentration on the% removal of Ni ions using (Manganese Ferrite) at pH 6, adsorbent dosage 2 g/l and temperature 25°C

The influence of contact time on the adsorption of Eosin color using a batch reactor is shown in Figs. 9-13. The results reveal that by expanding the contact time and the Eosin color concentration, the adsorption capacity rises [33]. It is also shown that the quantity of dye take-up is expanded with expanding contact time at all introductory color concentrations. Moreover, the dye adsorbed is expanded with the raise in the starting dye concentration. Those findings prove that the starting color concentration has no impact on the desired time for balance. The adsorption rate is higher at the start time because of the presence of the empty spots at the starting stage since there is a rise in the concentration gradients between the solution adsorbate and the surface adsorbate. With the passing of time, the color concentration decreases because of the concentrated dye inside the empty spots, and hence diminishing the adsorption rate in subsequent stages (Vadivelan and Kumar 2005) [34].

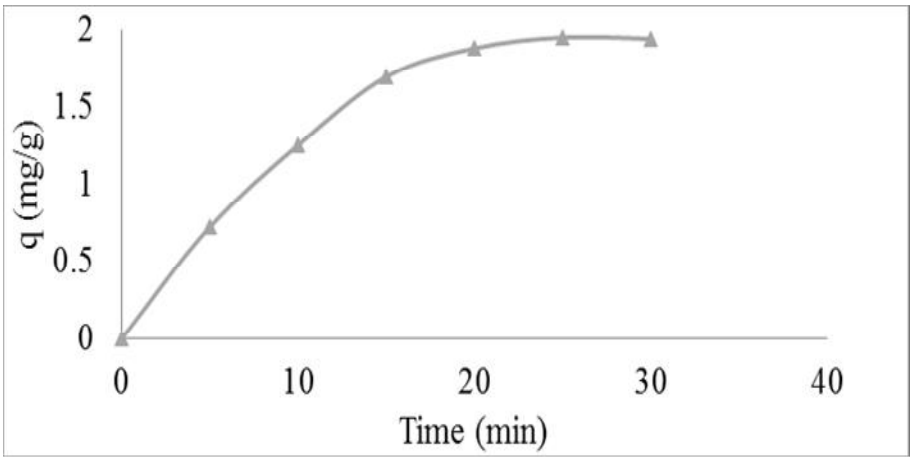

Fig. 9. Influence of contact time on the adsorption capacity of (Manganese ferrite) for Eosin dye at 50 ppm concentration and pH 6, adsorbent dosage 2 g/l and temperature 25°C

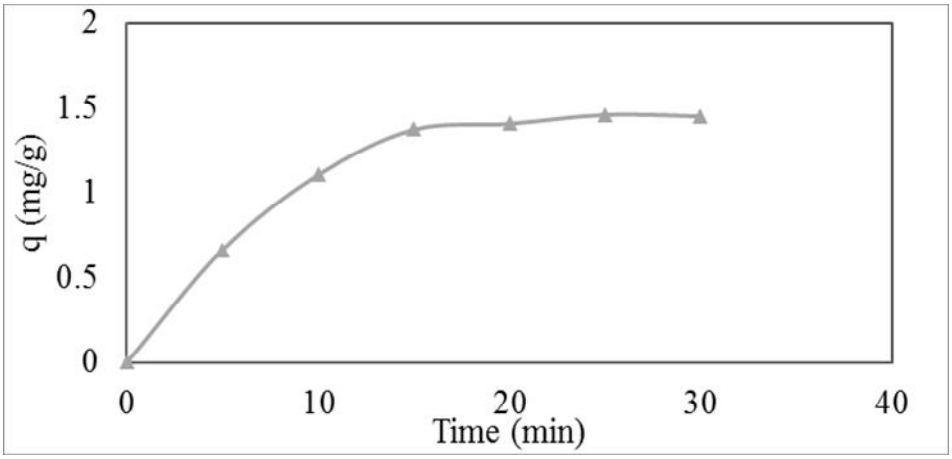

Fig. 10. Influence of contact time and Ni concentration on the adsorption capacity of (Manganese ferrite) for Eosin dye at 30 ppm concentration and pH 6, adsorbent dosage 2 g/l and temperature 25°C

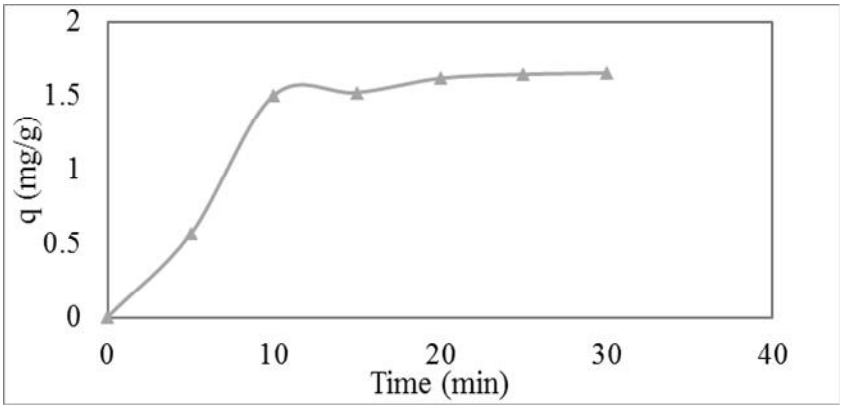

Fig. 11. Influence of contact time on the adsorption capacity of (Manganese ferrite) for Eosin dye at 20 ppm concentration and pH 6, adsorbent dosage 2 g/l and temperature 25°C

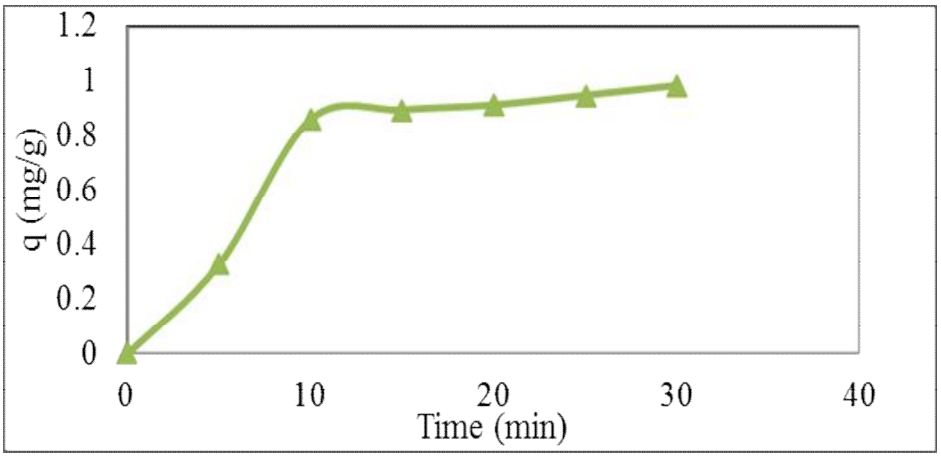

Fig. 12. Influence of contact time on the adsorption capacity of (Manganese ferrite) for Eosin dye at 10 ppm concentration and pH 6, adsorbent dosage 2 g/l and temperature 25°C

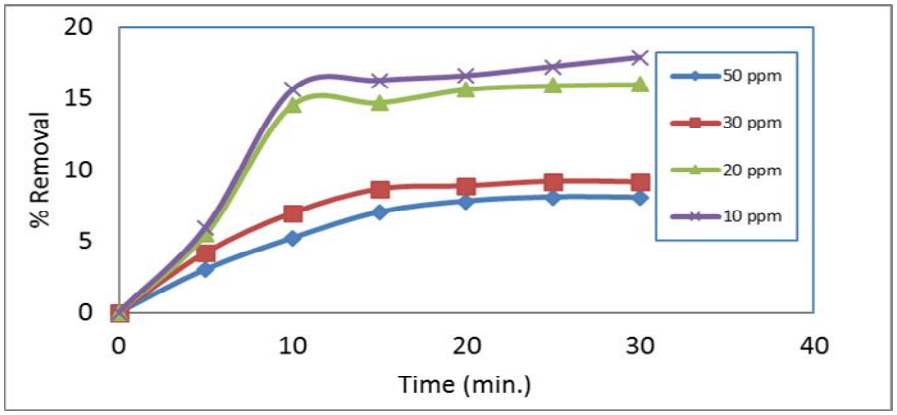

Fig. 13. Influence of contact time on the % removal of (Manganese ferrite) for Eosin dye at different concentrate adsorbent dosage 2 g/l and temperature 25°C

3.3 Influence of pH

To prepare 100 ppm of the tested solution:

1. Place 100ml of the prepared solution in 3 bottles.
2. Change the pH to 2, 4 and 8 respectively.
3. Add 0.4 g of manganese ferrite to each bottle. Then, place the bottles in a shaker operating at 220 rpm for half an hour. [35, 36]

The solution's acidity (pH) is the most imperative parameter responsible for the removal of heavy metals from fluids. Aiming at optimizing the pH for the highest effective removal, tests at 25^{o} C are made by adding 100 mL of 100 ppm Ni^{+2} solution to 1g/l of manganese oxide Nano powder and contact time (1/2 hour) and constantly blending and adjusting the solution pH with HCl and NaOH solutions at chosen pH values of 2, 4, 6 and 8.

Fig. 14 reveals the pH's impacts on the adsorption of Ni^{+2}. Ni^{+2}'s adsorption is considered as the most desirable when the introductory solution pH is between 2 and 8. The result confirms that as the pH of the water solution rises, the percent removal of Nickel is increased. [37] Therefore, by raising the pH, the electrostatic shock is decreased due to the decrease of the positive charge thickness at the adsorption spots, and this could boost the adsorption of metal ions. [38]

Fig. 15 reveals the pH's impact on the adsorption of Eosin dye. The adsorption of Eosin color is proven to be desirable when the initial solution pH is less than 6. [39]

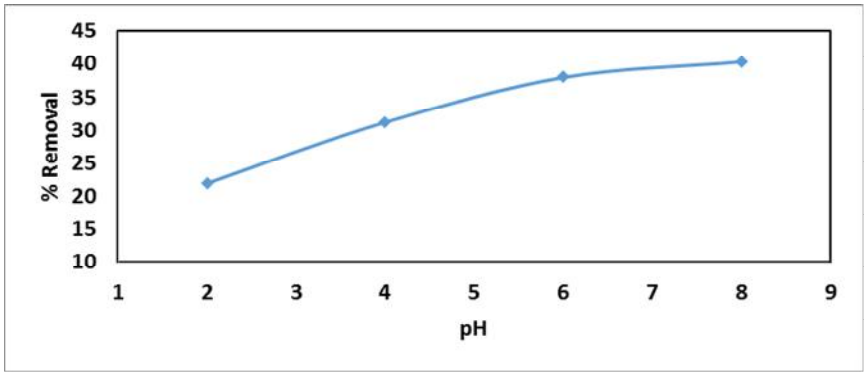

Fig. 14. Influence of pH on the removal of Ni (II) at 100 ppm initial concentration, 2g/l adsorbent dosage and at 25 C for 1/2 hour

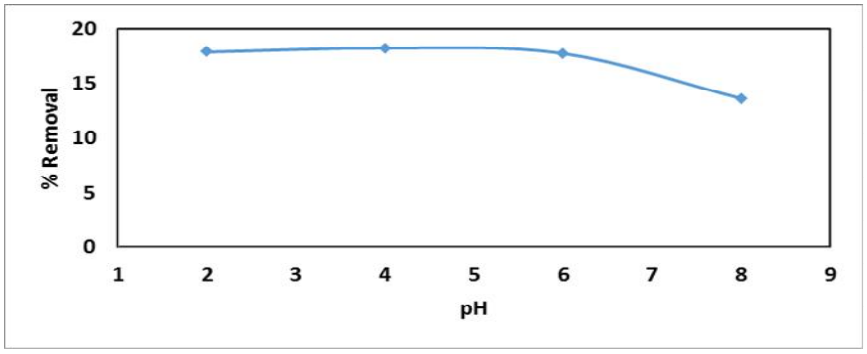

Fig. 15. Influence of pH on the removal of Eosin Dye at 10 ppm initial concentration, 2g/l adsorbent dosage and at 25°C for 1/2 hour.

3.4. Influece of adsorbent weight

To prepare a 100 ppm nickel solution, 100 ml of the solution is put in 3 bottles. 0.2, 0.3 and 0.4 g of manganese ferrite are added to each bottle in order. Then, the bottles are put inside a shaker working at 220 rpm for half an hour [35,36].

The tests results of different adsorbent concentrations are displayed in Figs. 16 and 17. It is noticed that as the concentration of the adsorbent is increased from 1 to 3 g/L, the removal of Ni 2+ is increases in turn from 37% to 60% in the batch reactor. Moreover, as the adsorbent dose rises from 1 to 4 g/L, the removal of Eosin yellow rises from 12% to 28% in the batch reactor. These results are in consensus with those of previous studies. [40]

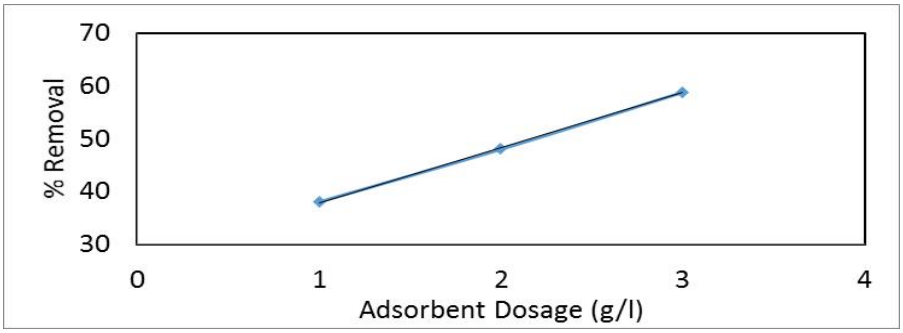

Fig. 16. Influence of adsorbent dosage on the removal of Ni (II) at 100 ppm initial concentration, 6 pH and at 25° C for 1/2 hour

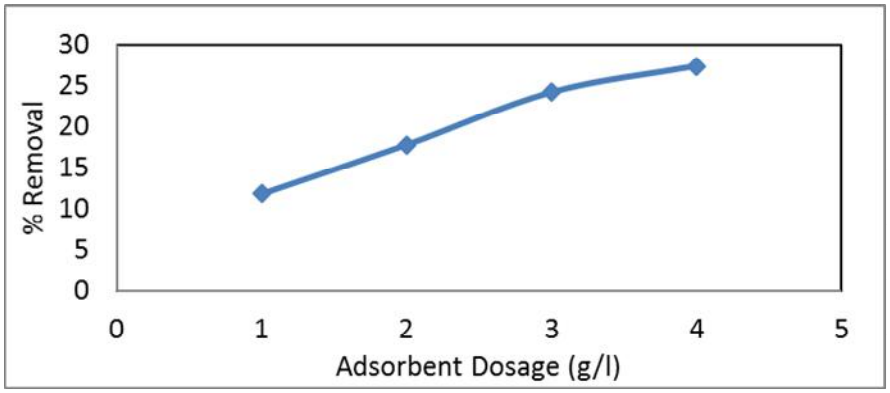

Fig. 17. Influence of adsorbent dosage on the removal of Eosine dye at 10 ppm initial concentration, 6 pH and at 25° C for 1/2 hour

3.5 Kinetics of adsorption

3.5.1 Pseudo-first-order equation

The adsorption kinetics data is accounted for by the Lagergren pseudo-first-order model; [41] the first equation to account for the adsorption rate based on the adsorption capacity. The linear form equation is com0monly represented as follows:

$$ln(q_e - q_t) = lnq_e - Kt \quad (8)$$

To calculate the rate constants, the values of ln (qe −qt) are linearly correlated with t by plot of ln (qe −qt) vs. t to yield a linear relationship from which K1 and predicted qe can be plotted from the slope and intercept.

3.5.2 Pseudo-second-order equation

The adsorption kinetic can be accounted for by the pseudo-second order model. The linear equation is commonly represented as follows:

$$\frac{t}{q_t} = \frac{1}{K_2}\frac{1}{q_e^2} + \frac{1}{q_e}t \quad (9)$$

If the second-order kinetics is applicable, then the plot of t/qt vs. t expresses a linear relationship. Values of K_2 and equilibrium adsorption capacity q_e are calculated from the intercept and slope of the plots of t/q_t vs. t. The linear plots of t/qt vs. t are in consensus with both experimental and calculated q_e values (Table 2). The correlation coefficients for the pseudo second-order kinetic model are greater than 0.95, which concludes that the pseudo second order kinetic model provides good correlation for the adsorption of Ni^{2+} and Eosin dye onto Manganese ferrite.

The adsorbate transferred from the bulk solution phase to the internal active slots takes place across a number of steps, where the rate of internal mass transfer is most often the rate-determining step in adsorption processes. Kinetic data is used next to test the occurrence of intra-particle diffusion using the Weber and Morris equation shown in the following equation;

$$qt = k_d\, t^{0.5} + c \quad (10)$$

Where q_t (mg g^{-1}) is the quantity of adsorbed Ni^{2+} at time t, and k_d is the intra-particle diffusion rate constant ($mg.g^{-1}$ $min^{-0.5}$), and c is a constant determined from the intercept. If the plot of (q_t) vs. ($t^{1/2}$) yields a straight line passing through the origin, then the adsorption process is only controlled by intra-particle diffusion, if multi-linearity in qt vs. t1/2 plot is considered (that is, two or three steps are involved to follow the whole process). Figs. 18 and 19 show that the external surface adsorption appears in the first step, and that the gradual adsorption step is the second step, where intraparticle diffusion is controlled; and that the final equilibrium step is the third step where the solute moves gradually from the bigger pores to micropores, resulting in a slow adsorption rate. [42]

Table 2. Kinetic parameters for the adsorption of Ni 2+ and Eosin dye onto manganese ferrite

Conc. (ppm)	Pseudo first-order kinetics			Pseudo second-order kinetics		
	K_1 (min^{-1})	q_1 (mg g^{-1})	R^2	K_2 (g $mg^{-1}min^{-1}$)	q_2 (mg g^{-1})	R^2
100 -Ni(II)	0.0643	22.693	0.9801	0.0047	27.77	0.9965
75 - Ni(II)	0.0403	11.078	0.9416	0.1273	1.326	0.9483
50 - Dye	0.1391	2.2988	0.962	0.0249	2.973	0.9595
30 – Dye	0.1273	1.326	0.9483	0.208	2.5694	0.9333

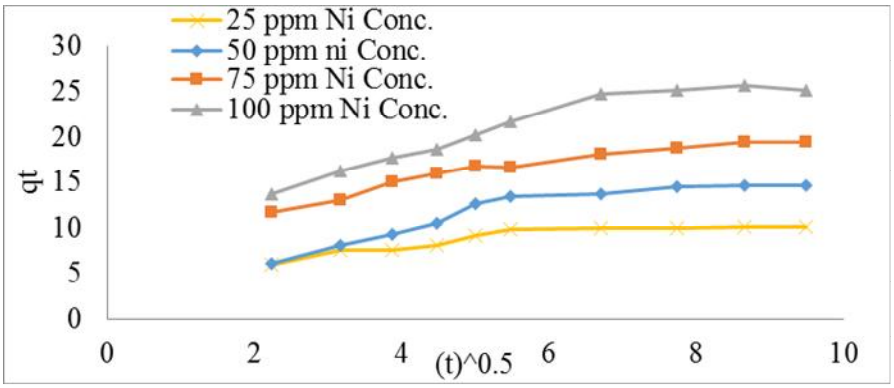

Fig. 18. Intra-particle diffusion test for adsorption of Ni at varying concentrations by Manganese Ferrite using batch reactor

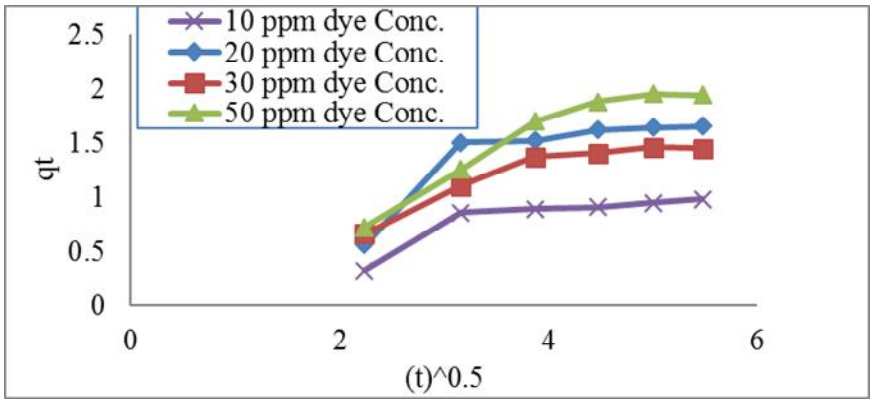

Fig. 19. Intra-particle diffusion test for adsorption of Eosin Dye at varying concentrations by Manganese Ferrite using batch reactor

4. CONCLUSION

The experimental data has shown that Nano manganese ferrite can be adopted and used as a good adsorbent for the removal of nickel and Eosin yellow from waste water.

1. Ni (II) removal increases by increasing contact time.
2. Ni (II) removal reaches 82% for 25 ppm by using ½ gram nano-manganese ferrite for 90 min.
3. Ni (II) removal increases by increasing pH (2-8) of solution and weight of adsorbent.
4. Eosin yellow removal increases by increasing contact time.
5. Eosin yellow removal reaches 18% for 10 ppm using ½ gram of nano manganese ferrite for 30 min.
6. Eosin yellow removal decreases by increasing pH (2-8) and increases by increasing the weight of adsorbent.
7. The Langmuir and Freundlich models are the most commonly agreed upon surface

adsorption models for single-solute systems.

COMPETING INTERESTS

Author has declared that no competing interests exist.

REFERENCES

1. Bradl, Heike, ed. Heavy metals in the environment: origin, interaction and remediation. Elsevier; 2005.
2. Available:https://www.slideshare.net/NehaKumar09/impact-of-the-dye-industry-on-the-environment.
3. Acharya, Seema, Babulal Rebery. "Fluorescence spectrometric study of eosin yellow dye–surfactant interactions." Arabian Journal of Chemistry. 2009;2.1:7-12.
4. Jain, Akshay, Rajasekhar Balasubramanian, Srinivasan MP. "Hydrothermal conversion of biomass waste to activated carbon with high porosity: A review." Chemical Engineering Journal. 2016;(283):789-805.
5. Available:http://www.theprojectdefinition.com/adsorption/
6. Abbas, Aamir, et al. "Heavy metal removal from aqueous solution by advanced carbon nanotubes: critical review of adsorption applications." Separation and Purification Technology. 2016(157):141-161.
7. Piao, Wenhua, et al. "Life cycle assessment and economic efficiency analysis of integrated management of wastewater treatment plants." Journal of Cleaner Production. 2016;(113):325-337.
8. Cheng Z, Tan ALK, Tao Y, Shan D, Ting KE, Yin XJ. Synthesis and characterization of iron oxide nanoparticles and applications in the removal of heavy metals from industrial wastewater. International Journal of Photoenergy; 2012.
9. Mahmoud AM, Ibrahim FA, Shaban SA, Youssef NA. Adsorption of heavy metal ion from aqueous solution by nickel oxide nano catalyst prepared by different methods. Egyptian Journal of Petroleum. 2015;24(1):27-35.35.
10. Ghiloufi IMED, Imam A, Saud M. "Effect of indium concentration in zinc oxide nanoparticles on heavy metals adsorption from aqueous solution." Recent Advances in Circuits, Communications and Signal Processing; 2013.
11. Du, Jingjing, Chuanyong Jing. "Preparation of Fe3O4@ Ag SERS substrate and its application in environmental Cr (VI) analysis." Journal of Colloid and Interface Science. 2011;(358.1):54-61.
12. Singh, Sarika, Barick KC, Bahadur D. "Surface engineered magnetic nanoparticles for removal of toxic metal ions and bacterial pathogens." Journal of Hazardous Materials. 2011;(192.3):1539-1547.
13. Liu, Jing-Fu, Zong-shan Zhao, and Gui-bin Jiang. "Coating Fe3O4 magnetic nanoparticles with humic acid for high efficient removal of heavy metals in water." Environmental science & technology 2008: (42.18): 6949-6954.
14. Chou, Chih-Ming, Hsing-Lung Lien. "Dendrimer-conjugated magnetic nanoparticles for removal of zinc (II) from aqueous solutions." Journal of Nanoparticle Research. 2011(13.5):2099-2107.
15. Ghaniem R, El-Taweil YA, Ossman ME. "Use of hydrous manganese oxides Nanopowders as a potential sorbent for selective removal of nickel ions from industrial waste water, kinetics and isotherm studies." Am. J. Chem. Eng. 2016;(4.6):170-178.
16. Mahmoodi, Niyaz Mohammad, Masoomeh Banijamali, Babak Noroozi. "Surface modification and ternary system dye removal ability of manganese ferrite nanoparticle." Fibers and Polymers. 2014;15.8:1616-1626.
17. Hankare PP, et al. "Gas sensing properties of magnesium ferrite prepared by co-precipitation method." Journal of Alloys and Compounds. 2009;(488.1):270-272.
18. Shahbeig, Hossein, et al. "A new adsorption isotherm model of aqueous solutions on granular activated carbon." World Journal of Modelling and Simulation. 2013;(9.4):243-254.
19. Hassaan, Mohamed A., Ahmed El Nemr, Fedekar F. Madkour. "Testing the advanced oxidation processes on the degradation of Direct Blue 86 dye in wastewater." The Egyptian Journal of Aquatic Research. 2017;(43.1):11-19.
20. Gupta, Vinod Kumar, et al. "Chemical treatment technologies for waste-water recycling—an overview." Rsc Advances. 2012;(2.16):6380-6388.
21. Zendehdel M, et al. "Removal of methylene blue dye from wastewater by adsorption

onto semi-inpenetrating polymer network hydrogels composed of acrylamide and acrylic acid copolymer and polyvinyl alcohol. 2010;423-428.
22. Huang, Chen-Chia, and Shu-Fang Siao."Removal of copper ions from an aqueous solution containing a chelating agent by electrosorption on mesoporous carbon electrodes. Journal of the Taiwan Institute of Chemical Engineers. 2018;(85):29-39.
23. Liu Jian, et al. "Progress in adsorption-based CO2 capture by metal–organic frameworks." Chemical Society Reviews. 2012;(41.6):2308-2322.
24. Fomina Marina, Geoffrey Michael Gadd. "Biosorption: current perspectives on concept, definition and application." Bioresource Technology. 2014;(160):3-14.
25. Gadkari AB, Shinde TJ, Vasambekar PN, Structural and magnetic properties of nanocrystalline Mg–Cd ferrites prepared by oxalate co-precipitation method, J Mater Sci. Mater Electron. 2010;21(1):96-103.
26. Josyulu OS, Sobhanadri J. The far-infrared spectra of some mixed cobalt zinc and magnesium zinc ferrites, Phys Status Solid. 1981;A,65(2):479–483.
27. Gadkari AB, Shinde TJ, Vasambekar PN. "Structural and magnetic properties of nanocrystalline Mg–Cd ferrites prepared by oxalate co-precipitation method." Journal of Materials Science: Materials in Electronics. 2010;(21.1):96-103.
28. Maensiri, Santi, Montana Sangmanee, Amporn Wiengmoon. "Magnesium ferrite (MgFe 2 O 4) nanostructures fabricated by electrospinning." Nanoscale Research Letters. 2009(4.3):221-228.
29. Wu, Yihan. "Environmental remediation of heavy metal ions by novel-nanomaterials: A review." Environmental Pollution. 2019(246):608-620.
30. Oliveira, Sílvia C, Marcos von Sperling. "Performance evaluation of different wastewater treatment technologies operating in a developing country." Journal of Water, Sanitation and Hygiene for Development. 2011(1.1):37-56.
31. Guo J, Song Y, Ji X, Ji L, Cai L, Wang Y, Zhang H, Song W. Preparation and characterization of nanoporous activated carbon derived from prawn shell and its application for removal of heavy metal ions. Materials. 2019;12:241.
DOI: 10.3390/ma12020241.
32. Huang Y, Li S, Chen J, Zhang X, Chen Y. Adsorption of Pb (II) on mesoporous activated carbons fabricated from water hyacinth using H3PO4 activation: Adsorption capacity, kinetic and isotherm studies. Appl. Surf. Sci. 2014;293:160–168.
33. Rezk, Marwan Y, et al. "Robust photoactive nanoadsorbents with antibacterial activity for the removal of dyes." Journal of Hazardous Materials. 2019(378):120679.
34. Vadivelan V, Kumar KV. Equilibrium, kinetics, mechanism, process design for the sorption of Methylene blue onto rice husk. J Colloid Interface Sci. 2005;(286):90–100.
35. Tu YJ, Chan TS, Tu HW, Wang SL, You CF, Chang CK. Rapid and efficient removal/recovery of molybdenum onto ZnFe2O4 Nanoparticles, Chemosphere. 2016;(148):452–458.
36. Tu, Yao-Jen, et al. "Efficient removal/recovery of Pb onto environmentally friendly fabricated copper ferrite nanoparticles." Journal of the Taiwan Institute of Chemical Engineers. 2017;(71):197-205.
37. Ahmaruzzaman, Md. "Nano-materials: Novel and Promising Adsorbents for Water Treatment." Asian Journal of Water, Environment and Pollution. 2019(16.3):43-53.
38. Hannachi Y, Shapovalov NA, Hannachi A. Adsorption of Nickel from aqueous solution by the use of low-cost adsorbents. Korean J. Chem. Eng. 2010;27:152–158.
DOI: 10.1007/s11814-009-0303-7.
39. Mahmoodi-Babolan, Negin, Amir Heydari, Ali Nematollahzadeh. "Removal of methylene blue via bioinspired catecholamine/starch superadsorbent and the efficiency prediction by response surface methodology and artificial neural network-particle swarm optimization." Bioresource Technology. 2019(294):122084.
40. Almomani, Fares, et al. "Heavy metal ions removal from industrial wastewater using magnetic nanoparticles (MNP)." Applied Surface Science. 2020(506):144924.
41. Torabi, Mehrnoosh, et al. "A Hybrid clustering and classification technique for forecasting short-term energy consumption." Environmental Progress & Sustainable Energy. 2019;(38.1):66-76.

42. Tan KL, Hameed BH. "Insight into the adsorption kinetics models for the removal of contaminants from aqueous solutions." Journal of the Taiwan Institute of Chemical Engineers. 2017;(74):25-48.

Peer-review history:
The peer review history for this paper can be accessed here:
https://www.sdiarticle4.com/review-history/69583